Molecular Orientation Analysis of Alkyl Methylene Groups from Quantitative Coherent Anti-Stokes Raman Scattering Spectroscopy

ARTICLE *in* JOURNAL OF PHYSICAL CHEMISTRY LETTERS · MARCH 2015

Impact Factor: 7.46 · DOI: 10.1021/acs.jpclett.5b00394

4 AUTHORS, INCLUDING:

Chi Zhang
Purdue University
33 PUBLICATIONS **222** CITATIONS
SEE PROFILE

Joshua Jasensky
University of Michigan
24 PUBLICATIONS **139** CITATIONS
SEE PROFILE

THE JOURNAL OF PHYSICAL CHEMISTRY Letters

Letter

pubs.acs.org/JPCL

Molecular Orientation Analysis of Alkyl Methylene Groups from Quantitative Coherent Anti-Stokes Raman Scattering Spectroscopy

Chi Zhang,*[,†] Jie Wang,[†,§] Joshua Jasensky,[‡] and Zhan Chen[†]

[†]Department of Chemistry, and [‡]Department of Biophysics, University of Michigan, 930 North University Avenue, Ann Arbor, Michigan 48109, United States

Supporting Information

ABSTRACT: Quantitative data analysis in coherent anti-Stokes Raman scattering (CARS) spectroscopy is important for extracting molecular structural information. We developed a method to derive molecular tilt angle with respect to the surface normal based on quantitative CARS spectral analysis. We showed that the tilt angle of methylene alkyl chains on a surface can be directly obtained from the CH_2 symmetric/asymmetric peak ratio in a CARS spectrum. The lipid alkyl chain tilt angle from a lipid monolayer was measured to be ~0° and was verified by sum frequency generation spectroscopy, which probes the orientations of the lipid methyl end groups. The tilt angle of a silane monolayer alkyl chain was derived to be ~35°, which agrees with the theoretical prediction. This method is submonolayer sensitive and can also be used to interpret polarization-dependent signals in CARS microscopy. It can be applied to elucidate detailed molecular structure from CARS spectroscopic and microscopic measurements.

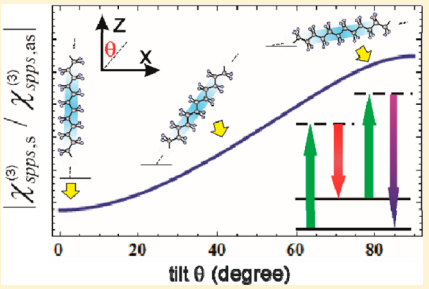

Since coherent anti-Stokes Raman scattering (CARS) vibrational spectroscopy has found important applications in biological and material research,[1−6] quantitative CARS spectral analysis has become an important step for the extensive understanding of experimental data and unveiling the physical information behind the spectra. One important consideration for quantitative CARS spectroscopy is to overcome spectral distortion caused by nonresonant background. Excellent research has shown the ability to acquire useful Raman information by effectively subtracting nonresonant CARS signal using various methods such as heterodyne detection,[7,8] maximum entropy method,[9−11] and a modified Kramers−Krönig transformation.[10,12,13] Another important direction of quantitative CARS microscopy is to sort spectral information into groups to derive chemical composition maps for complicated systems using methods such as principle component analysis,[14] hierarchical cluster analysis,[15] classical least-squares analysis,[16] and singular value decomposition analysis.[17] Additionally, since one of the most important advantages of vibrational spectroscopic techniques is the ability to elucidate complicated molecular structures based on quantitative spectral analysis, CARS has been used to study molecular orientations in a specimen. Research has shown the capability of deriving longitudinal ordering and orientation of molecules by using rotation polarization CARS (RPCARS).[18−23] However, currently, the derivation of molecular tilt angle (with respect to the surface normal) of molecules on surfaces/at interfaces using CARS has not been reported. For surface science and thin film studies, it is particularly important to obtain such tilt angle information on surface molecules/functional groups to understand surface properties.

We previously reported the quantitative interpretation of CARS responses of different methyl group vibrational modes based on molecular geometries and Raman measurements.[24] Using a bond additivity method, Raman and CARS responses of methyl groups have been theoretically derived and have shown good agreement with experimental results.[24] In this work, we developed a novel CARS data analysis method, capable of deriving orientation information on surface molecules. We first extended the bond additivity model to analyze the CARS spectra of methylene groups that possess C_{2v} symmetry, as well as that of the *trans*-alkyl chains. Additionally, we show that molecular tilt angle can be obtained from the methylene symmetric/asymmetric peak intensity ratio in a CARS spectrum.

Using RPCARS, only the angles of longitudinal aligned dipoles in reference to laser polarization can be measured.[18−23] In contrast, our method is able to extract molecular tilt angle with respect to the surface normal of an isotropic surface. More specifically, we showed that the tilt angle of a methylene alkyl chain from self-assembled monolayers (SAMs) can be derived. This alkyl chain orientation could not be measured using surface-sensitive sum frequency generation (SFG) spectroscopy due to the inversion symmetry of methylene groups present in lipid chains, which generates no SFG signal. On the other hand, SFG can be used to measure the orientation of methyl end groups, which can help verify the tilt angle deduced from CARS. The combined CARS and SFG spectroscopic study can provide more detailed structural information for thin films. The

Received: February 23, 2015
Accepted: March 24, 2015

DOI: 10.1021/acs.jpclett.5b00394
J. Phys. Chem. Lett. 2015, 6, 1369−1374

method presented in this work is widely applicable in CARS spectroscopy and microscopy for quantitative molecular structural analysis.

The CARS signal output is determined by the input lasers and the effective third order nonlinear susceptibility of the material $\chi^{(3)}_{\mathrm{eff}}$, which usually contains a resonant and a nonresonant components.[3] Under the condition of low nonresonant background, the following equation can be used to fit an experimentally measured CARS spectrum for quantitative analysis.[24]

$$\chi^{(3)}_{\mathrm{eff}} = \chi^{(3)}_{\mathrm{NR}} + \sum \frac{\mathbf{A}_{\mathrm{R}}}{\Omega_{\mathrm{R}} - (\omega_{\mathrm{p}} - \omega_{\mathrm{s}}) - i\mathbf{\Gamma}_{\mathrm{R}}} \tag{1}$$

Here $\chi^{(3)}_{\mathrm{NR}}$ includes all the nonresonant terms as a constant, and $\mathbf{A}_{\mathrm{R}}$, $\mathbf{\Gamma}_{\mathrm{R}}$, Ω_{R}, ω_{p}, ω_{s} are resonance strength of a Raman transition, line width of the Raman transition, vibrational frequency, input pump/probe beam frequency, and Stokes beam frequency, respectively. $\chi^{(3)}_{\mathrm{eff}}$ is further related to the local susceptibility $\chi^{(3)}_{IJKL}$ of the material through Fresnel coefficients (L factors; see Supporting Information II).[24,25] CARS experiments performed using different polarization combinations measure different susceptibility components. For example, according to the lab coordinate system defined in Figure 1a, $\chi^{(3)}_{\mathrm{eff},ssss}$ (s-polarized signal, s-polarized pump, s-polarized probe, s-polarized Stokes) measures $\chi^{(3)}_{yyyy}$, while $\chi^{(3)}_{\mathrm{eff},spps}$ measures $\chi^{(3)}_{yxxy}$ plus $\chi^{(3)}_{yzzy}$ (under surface or bulk isotropic assumption).[24] The local third-order nonlinear susceptibility of CARS can be correlated to the molecular hyperpolarizbility $\gamma^{(3)}_{ijkl}$ and $\gamma^{(3)}_{ikjl}$ through the equation[26]

$$\chi^{(3)}_{IJKL} = \frac{N}{2}\cdot\Big(\sum_{IJKL=x,y,z}\langle R_{Ii}R_{Jj}R_{Kk}R_{Ll}\rangle\gamma^{(3)}_{ijkl} + \sum_{IJKL=x,y,z}\langle R_{Ii}R_{Jk}R_{Kj}R_{Ll}\rangle\gamma^{(3)}_{ikjl}\Big) \quad ijkl = a, b, c \tag{2}$$

Here N is the number density of the material, and R is the element of transformation matrix from lab frame (x,y,z) to the molecular coordinate system (a,b,c). The angle brackets here indicate an ensemble average. Details of R and the rotation combination we chose in this study are stated in the Supporting Information III. The molecular orientation information lies in the angles defined in R, which include azimuthal angle ϕ, tilt angle θ, and twist angle ψ. The Euler angle definition for the methylene alkyl chain is shown in Figure 1c. Since the pump and probe frequencies are degenerate in CARS, $\chi^{(3)}_{IJKL}$ has contributions from both $\gamma^{(3)}_{ijkl}$ and $\gamma^{(3)}_{ikjl}$, corresponding to the two terms on the right-hand side of eq 2. For the susceptibility components $\chi^{(3)}_{yyyy}$, $\chi^{(3)}_{yxxy}$, and $\chi^{(3)}_{yzzy}$ measured in our experiment, the contributions from $\gamma^{(3)}_{ijkl}$ and $\gamma^{(3)}_{ikjl}$ are equal (Supporting Information IV). Therefore, eq 2 can be reduced to

$$\chi^{(3)}_{IJKL} = N\cdot\sum_{IJKL=x,y,z}\langle R_{Ii}R_{Jj}R_{Kk}R_{Ll}\rangle\gamma^{(3)}_{ijkl} \tag{3}$$

The third-order hyperpolarizability $\gamma^{(3)}_{ijkl}$ is defined by[26]

$$\gamma^{(3)}_{ijkl} = \frac{C_0}{\Omega_{\mathrm{R}} - (\omega_{\mathrm{p}} - \omega_{\mathrm{s}}) - i\mathbf{\Gamma}_{\mathrm{R}}}\alpha'_{ij}\alpha'_{kl} \tag{4}$$

Here α'_{ij} and α'_{kl} are Raman polarizability derivatives in reference to the normal mode coordinate, and C_0 is a constant. For peaks with similar width at vibrational resonance, eq 4 is reduced to

$$\gamma^{(3)}_{ijkl} = C\alpha'_{ij}\alpha'_{kl} \tag{5}$$

Here C is a constant. In order to obtain α' for a methylene group, a modified bond additivity model is used. The coordinate systems chosen for a single C−H bond and the entire CH_2 group are shown in Figure 1b and 1c, respectively. Figure 1d is the projection of Figure 1c on the $a-b$ plane shown for visual clarity. For a single C−H bond which possesses $C_{\infty v}$ symmetry, its Raman tensor derivative components satisfy $\alpha'_{aa}/\alpha'_{cc} = \alpha'_{bb}/\alpha'_{cc} = r$.[24] The value of r used in this work is discussed in the Supporting Information VII. The r value might be different for different molecular systems. The detailed analysis for deriving α' of the entire methylene group as well as the methylene alkyl chain using bond additivity method is presented in the Supporting Information V. For methylene group symmetric and asymmetric modes, we have

$$\boldsymbol{\alpha}'_s = b\times\alpha'_{cc}\begin{bmatrix} 0.477 + 0.937r & 0 & 0 \\ 0 & 0.937 + 0.477r & 0 \\ 0 & 0 & 1.414r \end{bmatrix} \tag{6a}$$

$$\boldsymbol{\alpha}'_{as} = \alpha'_{cc}\begin{bmatrix} 0 & -0.669 + 0.669r & 0 \\ -0.669 + 0.669r & 0 & 0 \\ 0 & 0 & 0 \end{bmatrix} \tag{6b}$$

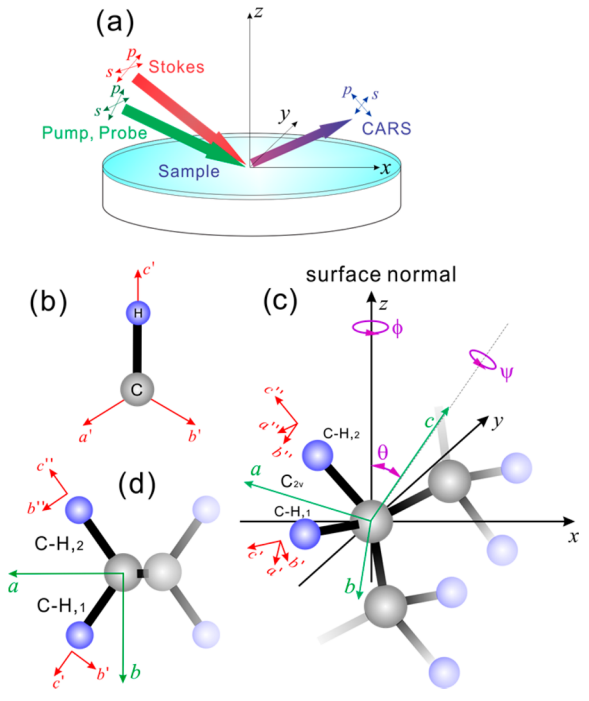

Figure 1. (a) CARS experimental geometry projected in the lab coordinate system (x,y,z) and defined for our analysis. Input and output lasers are in the $x-z$ plane. s and p polarizations are defined as perpendicular and parallel to the $x-z$ plane, respectively. (b) A single C−H bond and its molecular coordinate system (a',b',c'). (c) A methylene group in an alkyl chain and its molecular coordinate system chosen for analysis (a,b,c). The tilt, twist, and azimuthal angles for the alkyl chain (θ, ψ, and ϕ) are also defined. (d) The projection of the trans-arranged alkyl chain on the $a-b$ plane.

DOI: 10.1021/acs.jpclett.5b00394
J. Phys. Chem. Lett. 2015, 6, 1369−1374

In the conventional bond additivity method, the functional group under study is typically isolated from the entire molecule. Here, in order to take into the account of energy coupling of the methylene function group with bonds outside the group, as well as the possible energy coupling between the different vibrational modes, the ratio of symmetric and asymmetric Raman tensor derivatives needs to be modified. Therefore, in our modified bond additivity model, we introduce a factor b multiplying to the symmetric mode. This b value modifies the energy ratio between symmetric and asymmetric vibrational modes, and it can be obtained from CARS experimental measurements of bulk materials.[27]

Plugging these two equations into eqs 3 and 5, we can calculate all the components of the third order nonlinear susceptibility. Although $\chi^{(3)}$ has 81 elements, typically only a few of them are measured in CARS spectroscopy. To reduce the computational load, we use a method to separately calculate only the necessary components (Supporting Information IV). For the analysis of isotropic bulk materials, all azimuthal angles ϕ, tilt angles θ, and twist angles ψ need to be averaged. In doing so, we have

$$\chi^{(3)}_{IJKL} = \frac{C\cdot N}{4\pi^3}\int_0^{\pi}\int_0^{2\pi}\int_0^{2\pi} \mathbf{R}_I\boldsymbol{\alpha}'\mathbf{R}_J^T\mathbf{R}_K\boldsymbol{\alpha}'\mathbf{R}_L^T \sin\theta \, d\phi \, d\psi \, d\theta$$
$$IJKL = x, y, z \tag{7}$$

Here $\mathbf{R}$ is the $z-y-z$ transformation matrix shown in the Supporting Information III. $\mathbf{R}_x$, $\mathbf{R}_y$ and $\mathbf{R}_z$ are also defined as the first, second, and third rows of $\mathbf{R}$, respectively. For the surface molecule tilt angle analysis where the free twist rotation is assumed, we only average ϕ and ψ:

$$\chi^{(3)}_{IJKL}(\theta) = \frac{C\cdot N}{4\pi^2}\int_0^{2\pi}\int_0^{2\pi} \mathbf{R}_I\boldsymbol{\alpha}'\mathbf{R}_J^T\mathbf{R}_K\boldsymbol{\alpha}'\mathbf{R}_L^T \, d\phi \, d\psi$$
$$IJKL = x, y, z \tag{8}$$

For the methylene group symmetric and asymmetric modes, we have

$$\left|\frac{\chi^{(3)}_{IJKL,s}(\theta)}{\chi^{(3)}_{IJKL,as}(\theta)}\right| = \left|\frac{\int_0^{2\pi}\int_0^{2\pi}\mathbf{R}_I\boldsymbol{\alpha}_s'\mathbf{R}_J^T\mathbf{R}_K\boldsymbol{\alpha}_s'\mathbf{R}_L^T d\phi d\psi}{\int_0^{2\pi}\int_0^{2\pi}\mathbf{R}_I\boldsymbol{\alpha}_{as}'\mathbf{R}_J^T\mathbf{R}_K\boldsymbol{\alpha}_{as}'\mathbf{R}_L^T d\phi d\psi}\right|$$
$$IJKL = x, y, z \tag{9}$$

We first calculated the ratio of $|\chi^{(3)}_{yyyy,s}/\chi^{(3)}_{yyyy,as}|/b^2$ by averaging all three angles using Mathematica 7.0. It is found that the value of r affects this ratio (Figure S2); the bigger the value of r, the bigger the ratio $|\chi^{(3)}_{yyyy,s}/\chi^{(3)}_{yyyy,as}|/b^2$, which ranges from ~2 to 30, as r in the range from 0 to 0.5 (Figure S2). However, it is found that $|\chi^{(3)}_{yxxy,s}/\chi^{(3)}_{yxxy,as}|/b^2$ and $|\chi^{(3)}_{yzzy,s}/\chi^{(3)}_{yzzy,as}|/b^2$ are independent of r (Figure S3). This indicates r has impact on the symmetric/asymmetric peak ratio on *ssss* polarization but not on *spps* polarization. Similar results were found when only ϕ and ψ are averaged for surface molecules (Figure S6, S7 and S8). Using any r value between 0 and 0.5, we can obtain a same curve of $|\chi^{(3)}_{yxxy,s}/\chi^{(3)}_{yxxy,as}|/b^2$ or $|\chi^{(3)}_{yzzy,s}/\chi^{(3)}_{yzzy,as}|/b^2$ as a function of molecular tilt angle θ (Figure S7 and S8). After considering the Fresnel L factors, we can derive the value $|\chi^{(3)}_{spps,s}/\chi^{(3)}_{spps,as}|/b^2$ as a function of θ as shown in Figure S9. This theoretical curve indicates that the experimental value of $|\chi^{(3)}_{spps,s}/\chi^{(3)}_{spps,as}|/b^2$ can be used to obtain molecular tilt angle of methylene groups.

In order to get the value of b, CARS spectrum from bulk material needs to be measured, which is generated by molecules with random orientations. Using our analysis above and after integrating all the three angles in the *spps* polarization, we have $|\chi^{(3)}_{spps,s}/\chi^{(3)}_{spps,as}| \approx 0.49b^2$ for all allowed values of r (Figure S3). We measured CARS spectrum of DPPG lipid powder on a silica window. The experimental setup used in this paper has been published previously,[28] and detailed in the Supporting Information I. The CARS spectrum in *spps* polarization is shown in Figure 2a, possessing two peaks centered at ~2855

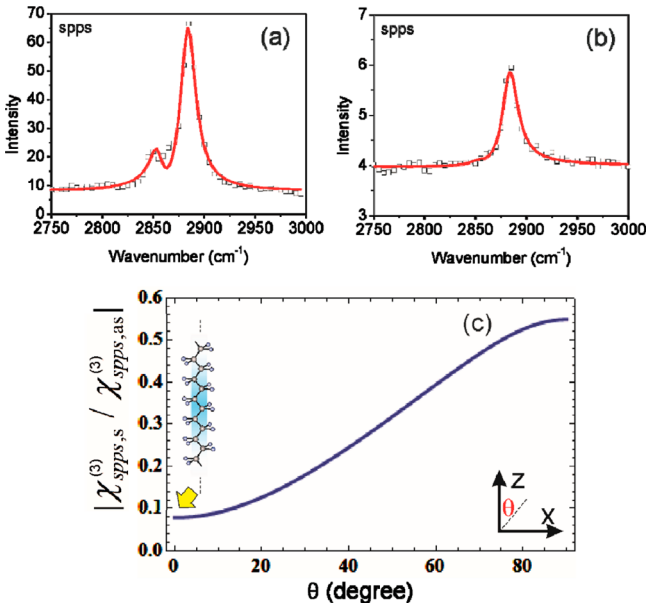

Figure 2. (a) CARS spectrum of DPPG powder collected using *spps* polarization combination. (b) CARS spectrum of a DPPG monolayer deposited on a silica window collected using *spps* polarization combination. Dots are experimental data, lines are spectral fitting results using eq 1. (c) The ratio of $|\chi^{(3)}_{spps,s}/\chi^{(3)}_{spps,as}|$ as a function of alkyl chain tilt angle θ, $b^2 \approx 0.67$.

and ~2883 cm^{-1}, corresponding to the symmetric and asymmetric stretching modes of methylene groups, respectively. Spectral fitting was performed using eq 1 and the results are shown in Table S2, which gives $|\chi^{(3)}_{spps,s}/\chi^{(3)}_{spps,as}| \approx 0.33$. From this we have that for DPPG molecule $b^2 \approx 0.67$. Using this value, the curve in Figure S9 is replotted as shown in Figure 2c, which can be used to analyze methylene group tilt angles of DPPG monolayer with the help of experimental data.

We deposited a DPPG monolayer on a silica window using the Langmuir–Blodgett method.[29] DPPG phase transition temperature is ~41 °C, and thus is in gel phase at room temperature. Under this condition, lipid alkyl chain methylene groups tend to adopt a trans-arrangement as we assumed in our calculation (Supporting Information V). The measured *spps* CARS spectrum is displayed in Figure 2b. From spectral fitting (Table S2) we have $|\chi^{(3)}_{spps,s}/\chi^{(3)}_{spps,as}| \approx 0.08$. On the curve in Figure 2c, this value corresponds to $\theta \approx 0°$. The results indicate that the lipid alkyl chain in the monolayer is likely "standing up" with small tilt angles.

To further verify our measurement and calculation of the methylene alkyl chain tilt angle, we used SFG spectroscopy to derive the molecular orientation of the methyl end groups. Different from CARS, SFG measures molecules where the centrosymmetry is broken.[30−33] Lipid alkyl chain has good inversion symmetry, which is usually SFG silent. However, methyl end groups from the alkyl chains do not have inversion

DOI: 10.1021/acs.jpclett.5b00394
J. Phys. Chem. Lett. 2015, 6, 1369−1374

symmetry and thus can be probed using SFG.[34] According to the previous CARS measurement of lipid alkyl chain adopting a very small tilt angle (~0°), the methyl end groups should thus adopt a tilt angle of ~35° (according to the molecular geometry of the tetrahedral carbon). We performed the SFG experiment on the same DPPG lipid monolayer using our original SFG spectrometer.

SFG spectrum of the lipid monolayer in *ssp* (*s*-polarized signal, *s*-polarized visible, *p*-polarized IR) polarization has three peaks: methyl symmetric stretching at ~2880 cm^{-1}, methyl Fermi resonance at ~2940 cm^{-1}, and methyl asymmetric stretching at ~2960 cm^{-1} (appears as a shoulder of the 2940 cm^{-1} peak, Figure 3a).[35] SFG spectral fitting was performed as

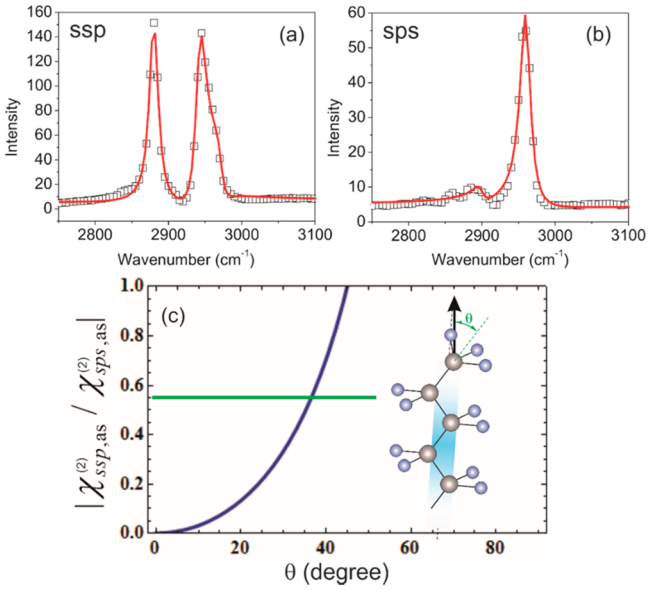

Figure 3. (a) SFG spectrum of a DPPG monolayer collected using *ssp* polarization combination. (b) SFG spectrum of a DPPG monolayer collected using *sps* polarization combination. Dots are experimental data, lines are fitting results using eq S19. (c) $|\chi^{(2)}_{ssp,as}/\chi^{(2)}_{sps,as}|$ as a function of methyl group tilt angle θ. The green line indicates the experimentally measured value.

shown in Figure 3a red curve, and the detailed fitting parameters are listed in Table S3. In *sps* polarization, strong peak at ~2960 cm^{-1} was detected and attributed to the methyl asymmetric stretching. Using the asymmetric stretching peaks under *ssp* and *sps* polarizations, the tilt angle θ of methyl end groups can be derived.[25,36] As detailed in the Supporting Information IX, we have $|\chi^{(2)}_{ssp,as}/\chi^{(2)}_{sps,as}| \approx |\chi^{(2)}_{yyz,as}/\chi^{(2)}_{yzy,as}| = 0.55$. Comparing this value with the theoretical curve of $|\chi^{(2)}_{ssp,as}/\chi^{(2)}_{sps,as}|$ as a function of θ shown in Figure 3c (assuming a delta tilt angle distribution), θ can be derived to be ~35°, which well matches our CARS measurement of lipid alkyl chains adopting ~0° tilt angle. If only SFG experiment was performed, from the ~35° methyl group tilt angle it is impossible to deduce the orientation of lipid alkyl chains due to the molecular rotation freedom along the methyl principle axis. Using CARS, we can directly measure the lipid alkyl chain orientation, which can help depict a clearer picture of surface molecular structures.

We also analyzed the tilt angle of alkyl chain from an octadecyltrimethoxysilane (OTMS) SAM grown on a silica substrate. The sample preparation is detailed in the Supporting Information X. The *spps* CARS spectrum from OTMS bulk was collected as shown in Figure S10a. From spectral fitting we have $b^2 \approx 1.18$. Using this value, and letting $\psi = 0$ (alkyl chain does not have rotation freedom in the OTMS SAM), we plot $|\chi^{(3)}_{spps,s}/\chi^{(3)}_{spps,as}|$ as a function of θ as shown in Figure S11. The *spps* CARS spectrum from the OTMS monolayer was displayed in Figures S10b. From spectral fitting we can derive $|\chi^{(3)}_{spps,s}/\chi^{(3)}_{spps,as}| \approx 0.38$, which corresponds to a tilt angle of ~35°. Based on the tetrahedral carbon geometry, this result matches the theoretical tilt angle (35°) when three Si−O bonds are connected to the substrate (Figure S12). It further implies the validity of our method for hydrocarbon chain orientation analysis on surfaces.

Polarized spontaneous Raman spectroscopy has been used to study the trend in alkyl chain orientation change in supported lipid bilayers.[37,38] By comparison, our work shows that CARS can provide specific tilt angle measurements of SAM molecules. Additionally, combining CARS and SFG spectroscopy on a single platform, we have the potential to obtain more detailed molecular structural information on thin films.[39] First of all, CARS and SFG might be sensitive for different moieties of a molecule, such as CH_2 and CH_3 groups in an alkyl chain. Additionally, for the same functional group, if its vibration modes are both IR and Raman active, SFG can measure tilt angle information on $\langle\cos\theta\rangle$ and $\langle\cos^3\theta\rangle$, and CARS can measure $\langle\cos^2\theta\rangle$ and $\langle\cos^4\theta\rangle$.[39,40] This indicates that if surface molecules tend to adopt multiple orientation distributions, the combined SFG and CARS spectroscopy might provide more detailed structural information. Although we believe that the alkyl chains of the SAMs used in this work tend to adopt a single tilt angle distribution, the combined spectroscopic study could be extended to characterize more complicated systems in the future.

As shown above, alkyl chain orientation in lipid monolayer can be derived using our method. Lipid bilayers serving as model membranes can be analyzed similarly. We extend our method to quantitatively analyze lipid membrane images in CARS microscopy. If we measure lipid vesicle CH_2 CARS signal using a tightly focused collinear CARS geometry as used in most implementations of CARS microscopy,[18] for the lipid alkyl chains orientated along the input beam polarizations (assuming all input beams having the same linear polarization), $\chi^{(3)}_{zzzz}$ is measured; for the alkyl chains orientated perpendicularly to the input beam polarizations, $\chi^{(3)}_{yyyy}$ is measured (Figure S13). Here we assume that the laser focal plane is at the center of the vesicle. Resetting our coordinate system, assuming that the lipid alkyl chains have zero tilt angle with respect to its surface normal and considering the transmission geometry (Supporting Information, XI), we can derive $|\chi^{(3)}_{zzzz,s}/\chi^{(3)}_{yyyy,s}| < 0.11$, when $r <$ 0.2 (Figure S14). Here only the CH_2 symmetric mode is considered since in *ssss* polarization the symmetric stretching is much stronger than the asymmetric stretching. Therefore, the lipid alkyl chains aligned parallelly with input polarization (area A, Figure S13) should have much lower CARS signal as compare to that aligned perpendicularly with input polarization (area B, Figure S13). Such phenomenon has been observed and reported by other groups.[18,23] Our analysis further indicates that for a lipid vesicle, the value of $|\chi^{(3)}_{zzzz,s}/\chi^{(3)}_{yyyy,s}|$ is *r*-dependent (Figure S14). For the lipid alkyl chain orientated in other radical angles, contributions from both $\chi^{(3)}_{zzzz}$ and $\chi^{(3)}_{yyyy}$ determine the signal strength, which is between the minimum and maximum signal conditions.

In this paper we used a bond additivity model to theoretically derive α', which can also be obtained from polarized spontaneous Raman experiment. However, using this model,

DOI: 10.1021/acs.jpclett.5b00394
J. Phys. Chem. Lett. 2015, 6, 1369−1374

no spontaneous Raman experiment is required for measuring α'. It is also shown that different α' resulted from different r values does not affect the orientation determination using polarized CARS. Our method further avoids possible error in determining α' using spontaneous Raman spectra caused by fitting overlapped C−H stretching Raman peaks.

In conclusion, we showed that CH_2 molecular orientation information can be measured directly using the symmetric and asymmetric C−H stretching peak ratio in a CARS spectrum collected in *spps* polarization. Lipid alkyl chain tilt angle from a DPPG monolayer deposited on a silica substrate was derived to be ∼0°. SFG experimental results further verified the CARS measurement. Additionally, alkyl chain tilt angle from an OTMS SAM was deduced to be ∼35° using CARS, well agreed with the theoretical value. Our method was also used to provide quantitative CARS signal analysis from lipid vesicle, capable of explaining polarization-dependent CARS intensity. This research provides in-depth insight for CARS spectral measurement and introduces a method to derive molecular tilt angles with respect to surface normal using CARS spectroscopy. It has the potential to help achieve a clearer understanding of molecular structures of complicated molecules on surfaces or in microscopy.

■ ASSOCIATED CONTENT

Supporting Information

(I) Experimental setup and sample preparation, (II) Fresnel factors, (III) transformation matrix **R**, (IV) calculation of third order nonlinear susceptibility components, (V) bond additivity calculation for Raman tensor derivatives of methylene group and methylene alkyl chain, (VI) CARS spectral fitting, (VII) calculation results of third order nonlinear susceptibility components, (VIII) fitting results of the SFG spectra, (IX) lipid methyl end group orientation analysis using SFG spectroscopy, (X) tilt angle analysis of alkyl chain from OTMS self-assembled monolayer, and (XI) lipid vesicle CARS signal analysis. This material is available free of charge via the Internet at http://pubs.acs.org.

■ AUTHOR INFORMATION

Corresponding Author

*E-mail: zhangchi@umich.edu; Tel: 734-389-5895.

Present Address

§(J.W.) AbbVie, 1 North Waukegan Road, North Chicago, Illinois, 60064, USA.

Notes

The authors declare no competing financial interest.

■ REFERENCES

(1) Zumbusch, A.; Holtom, G. R.; Xie, X. S. Three-Dimensional Vibrational Imaging by Coherent Anti-Stokes Raman Scattering. *Phys. Rev. Lett.* **1999**, *82*, 4142−4145.

(2) Volkmer, A.; Cheng, J.-X.; Xie, X. S. Vibrational Imaging with High Sensitivity via Epidetected Coherent Anti-Stokes Raman Scattering Microscopy. *Phys. Rev. Lett.* **2001**, *87*, 023901.

(3) Evans, C. L.; Xie, X. S. Coherent Anti-Stokes Raman Scattering Microscopy: Chemical Imaging for Biology and Medicine. *Annu. Rev. Anal. Chem.* **2008**, *1*, 883−909.

(4) Cheng, J.-X.; Xie, X. S. Coherent Anti-Stokes Raman Scattering Microscopy: Instrumentation, Theory, and Applications. *J. Phys. Chem. B* **2004**, *108*, 827−840.

(5) Duncan, M. D.; Reintjes, J.; Manuccia, T. Scanning Coherent Anti-Stokes Raman Microscope. *Opt. Lett.* **1982**, *7*, 350−352.

(6) Schmidt, S. C.; Moore, D. S. Vibrational Spectroscopy of High-Temperature, Dense Molecular Fluids by Coherent Anti-Stokes Raman Scattering. *Acc. Chem. Res.* **1992**, *25*, 427−432.

(7) Cheng, J.-X.; Book, L. D.; Xie, X. S. Polarization Coherent Anti-Stokes Raman Scattering Microscopy. *Opt. Lett.* **2001**, *26*, 1341−1343.

(8) Jurna, M.; Korterik, J.; Otto, C.; Herek, J.; Offerhaus, H. Vibrational Phase Contrast Microscopy by Use of Coherent Anti-Stokes Raman Scattering. *Phys. Rev. Lett.* **2009**, *103*, 043905.

(9) Rinia, H. A.; Bonn, M.; Müller, M.; Vartiainen, E. M. Quantitative CARS Spectroscopy Using the Maximum Entropy Method: The Main Lipid Phase Transition. *ChemPhysChem* **2007**, *8*, 279−287.

(10) Cicerone, M. T.; Aamer, K. A.; Lee, Y. J.; Vartiainen, E. Maximum Entropy and Time-Domain Kramers-Kronig Phase Retrieval Approaches Are Functionally Equivalent for CARS Microspectroscopy. *J. Raman Spectrosc.* **2012**, *43*, 637−643.

(11) Vartiainen, E. M.; Rinia, H. A.; Müller, M.; Bonn, M. Direct Extraction of Raman Line-Shapes from Congested CARS Spectra. *Opt. Express* **2006**, *14*, 3622−3630.

(12) Liu, Y.; Lee, Y. J.; Cicerone, M. T. Broadband CARS Spectral Phase Retrieval Using a Time-Domain Kramers−Kronig Transform. *Opt. Lett.* **2009**, *34*, 1363−1365.

(13) Day, J. P.; Domke, K. F.; Rago, G.; Kano, H.; Hamaguchi, H.-O.; Vartiainen, E. M.; Bonn, M. Quantitative Coherent Anti-Stokes Raman Scattering (CARS) Microscopy. *J. Phys. Chem. B* **2011**, *115*, 7713−7725.

(14) Lin, C.-Y.; Suhalim, J. L.; Nien, C. L.; MiljkoviÄ, M. D.; Diem, M.; Jester, J. V.; Potma, E. O. Picosecond Spectral Coherent Anti-Stokes Raman Scattering Imaging with Principal Component Analysis of Meibomian Glands. *J. Biomed. Opt.* **2011**, *16*, 021104−9.

(15) Arora, R.; Petrov, G. I.; Yakovlev, V. V. Hyperspectral Coherent Anti-Stokes Raman Scattering Microscopy Imaging through Turbid Medium. *J. Biomed. Opt.* **2011**, *16*, 021116−8.

(16) Lee, Y. J.; Moon, D.; Migler, K. B.; Cicerone, M. T. Quantitative Image Analysis of Broadband CARS Hyperspectral Images of Polymer Blends. *Anal. Chem.* **2011**, *83*, 2733−2739.

(17) Masia, F.; Glen, A.; Stephens, P.; Borri, P.; Langbein, W. Quantitative Chemical Imaging and Unsupervised Analysis Using Hyperspectral Coherent Anti-Stokes Raman Scattering Microscopy. *Anal. Chem.* **2013**, *85*, 10820−10828.

(18) Potma, E. O.; Xie, X. Detection of Single Lipid Bilayers with Coherent Anti-Stokes Raman Scattering (CARS) Microscopy. *J. Raman Spectrosc.* **2003**, *34*, 642−650.

(19) Wurpel, G.; Rinia, H.; Müller, M. Imaging Orientational Order and Lipid Density in Multilamellar Vesicles with Multiplex CARS Microscopy. *J. Microsc.* **2005**, *218*, 37−45.

(20) Wang, H.; Fu, Y.; Zickmund, P.; Shi, R.; Cheng, J.-X. Coherent Anti-Stokes Raman Scattering Imaging of Axonal Myelin in Live Spinal Tissues. *Biophys. J.* **2005**, *89*, 581−591.

(21) de Vito, G.; Bifone, A.; Piazza, V. Rotating-Polarization CARS Microscopy: Combining Chemical and Molecular Orientation Sensitivity. *Opt. Express* **2012**, *20*, 29369−29377.

(22) Minamikawa, T.; Takagi, T.; Niioka, H.; Kurihara, M.; Hashimoto, N.; Araki, T.; Hashimoto, M. Molecular Orientation Imaging of Liquid Crystals by Tunable-Polarization-Mode Coherent Anti-Stokes Raman Scattering Microscopy. *Appl. Phys. Express* **2013**, *6*, 072401.

(23) Kennedy, A. P.; Sutcliffe, J.; Cheng, J.-X. Molecular Composition and Orientation in Myelin Figures Characterized by Coherent Anti-Stokes Raman Scattering Microscopy. *Langmuir* **2005**, *21*, 6478−6486.

(24) Zhang, C.; Wang, J.; Ding, B.; Jasensky, J. Quantitative Spectral Analysis of Coherent Anti-Stokes Raman Scattering Signal: C−H Stretching Modes of the Methyl Group. *J. Phys. Chem. B* **2014**, *118*, 7647−7656.

(25) Zhuang, X.; Miranda, P.; Kim, D.; Shen, Y. Mapping Molecular Orientation and Conformation at Interfaces by Surface Nonlinear Optics. *Phys. Rev. B* **1999**, *59*, 12632−12640.

(26) Davis, R. P.; Moad, A. J.; Goeken, G. S.; Wampler, R. D.; Simpson, G. J. Selection Rules and Symmetry Relations for Four-Wave

DOI: 10.1021/acs.jpclett.5b00394
J. Phys. Chem. Lett. 2015, 6, 1369−1374

Mixing Measurements of Uniaxial Assemblies. *J. Phys. Chem. B* **2008**, *112*, 5834−5848.
(27) Hirose, C.; Akamatsu, N.; Domen, K. Formulas for the Analysis of Surface Sum-Frequency Generation Spectrum by Ch Stretching Modes of Methyl and Methylene Groups. *J. Chem. Phys.* **1992**, *96*, 997−1004.
(28) Zhang, C.; Wang, J.; Khmaladze, A.; Liu, Y.; Ding, B.; Jasensky, J.; Chen, Z. Examining Surface and Bulk Structures Using Combined Nonlinear Vibrational Spectroscopies. *Opt. Lett.* **2011**, *36*, 2272−2274.
(29) Tamm, L. K.; McConnell, H. M. Supported Phospholipid Bilayers. *Biophys. J.* **1985**, *47*, 105−113.
(30) Shen, Y. R. Surface Properties Probed by Second-Harmonic and Sum-Frequency Generation. *Nature* **1989**, *337*, 519−525.
(31) Lambert, A. G.; Davies, P. B.; Neivandt, D. J. Implementing the Theory of Sum Frequency Generation Vibrational Spectroscopy: A Tutorial Review. *Appl. Spectrosc. Rev.* **2005**, *40*, 103−145.
(32) Chen, Z.; Shen, Y. R.; Somorjai, G. A. Studies of Polymer Surfaces by Sum Frequency Generation Vibrational Spectroscopy. *Annu. Rev. Phys. Chem.* **2002**, *53*, 437−465.
(33) Zhang, C.; Myers, J. N.; Chen, Z. Elucidation of Molecular Structures at Buried Polymer Interfaces and Biological Interfaces Using Sum Frequency Generation Vibrational Spectroscopy. *Soft Matter* **2013**, *9*, 4738−4761.
(34) Liu, J.; Conboy, J. C. Direct Measurement of the Transbilayer Movement of Phospholipids by Sum-Frequency Vibrational Spectroscopy. *J. Am. Chem. Soc.* **2004**, *126*, 8376−8377.
(35) Zhang, C.; Wu, F.-G.; Hu, P.; Chen, Z. Interaction of Polyethylenimine with Model Cell Membranes Studied by Linear and Nonlinear Spectroscopic Techniques. *J. Phys. Chem. C* **2014**, *118*, 12195−12205.
(36) Wang, J.; Chen, C.; Buck, S. M.; Chen, Z. Molecular Chemical Structure on Poly(methyl methacrylate) (PMMA) Surface Studied by Sum Frequency Generation (SFG) Vibrational Spectroscopy. *J. Phys. Chem. B* **2001**, *105*, 12118−12125.
(37) Lee, C.; Bain, C. D. Raman Spectra of Planar Supported Lipid Bilayers. *Biochim. Biophys. Acta* **2005**, *1711*, 59−71.
(38) Woods, D. A.; Bain, C. D. Total Internal Reflection Raman Spectroscopy. *Analyst* **2012**, *137*, 35−48.
(39) Wang, J.; Paszti, Z.; Clarke, M. L.; Chen, X.; Chen, Z. Deduction of Structural Information of Interfacial Proteins by Combined Vibrational Spectroscopic Methods. *J. Phys. Chem. B* **2007**, *111*, 6088−6095.
(40) Chen, X.; Wang, J.; Boughton, A. P.; Kristalyn, C. B.; Chen, Z. Multiple Orientation of Melittin inside a Single Lipid Bilayer Determined by Combined Vibrational Spectroscopic Studies. *J. Am. Chem. Soc.* **2007**, *129*, 1420−1427.

DOI: 10.1021/acs.jpclett.5b00394
J. Phys. Chem. Lett. 2015, 6, 1369−1374